Society of Petroleum Engineers

SPE-189754-MS

General Analytical Model for Thermal-Solvent Assisted Gravity Drainage Recovery Processes

Hamed Reza Motahhari and Rahman Khaledi, Imperial Oil

This paper was prepared for presentation at the SPE Canada Heavy Oil Technical Conference held in Calgary, Alberta, Canada, 13-14 March 2018.

Abstract

Thermal-Solvent Assisted Gravity Drainage are recovery processes in which the stimulation mechanism for bitumen viscosity reduction is by heating and/or dilution. Different gravity drainage recovery processes can be included in this category depending on the range of the injection temperature and the solvent concentration in the injection stream. Examples are SAGD, SA-SAGD, VAPEX and heated VAPEX. The performance behavior of these processes is significantly driven by the complex thermodynamic interaction of steam and solvent, heat transfer, multiphase fluid equilibrium and flow in the porous medium.

In this study, we develop a general analytical model for gravity drainage processes by incorporating mass transfer mechanisms (including diffusion and dispersion) and heat transfer mechanism by conduction. In particular, we incorporate the dependency of diffusion and dispersion coefficients on concentration, temperature and drainage velocities, respectively. We utilize a novel approach to analytically solve the second order non-linear partial differential equation which governs mass transfer within the mass boundary layer. The resulted closed-form analytical model provides oil drainage rate due to gravity and heat and dilution effects as a function of reservoir and fluid properties. The developed model in this work provides a new perspective into the mass transfer mechanisms and their relative importance within the mass transfer boundary layer at different operating conditions.

The consistent application of the new model to the gravity drainage processes ranging from SAGD to VAPEX demonstrated using laboratory data from literature. It is shown that the predicted concentration distribution profile by the model with the concentration-dependent diffusion coefficient is profoundly different than the predicted profiles with a constant diffusion coefficient. The modeling results demonstrate that the dispersion can be several orders of magnitude greater than diffusion for solvent assisted gravity drainage process at the elevated temperatures. In addition, the contribution of the mass transfer boundary layer to oil production rate can be significantly greater than the heat transfer boundary layer despite being considerably narrower than the heat transfer boundary layer at the elevated temperatures. These findings confirms that the performance of solvent assisted gravity drainage process can be more favorable at the elevated temperatures.

Introduction

Bitumen and extra heavy oils are naturally occurring heavy hydrocarbon resources with extremely high viscosities at the reservoir pressure and temperature conditions. Enhanced oil recovery (EOR) methods are generally utilized to deliver heat and/or solvents to these in-situ resources to reduce the bitumen or heavy oil viscosity by increasing process temperature and/or dilution, respectively. A drive mechanism such as gravitational potential difference is required to flow the mobilized bitumen or heavy oil to the production well. Roger Butler was the pioneer to introduce the concept of the gravity drainage recovery process for bitumen and heavy oil extraction from Canadian oil sands in 1970s when he tested Steam Assisted Gravity Drainage (SAGD) at Imperial Oil's research center and piloted SAGD for the first time at Cold Lake (Butler 1979 and Butler et al. 1981). Furthermore, Butler and Mokrys (1989) developed an analog process to SAGD, in which a liquid solvent (toluene) was injected to reduce the bitumen viscosity. Butler and Mokrys (1989) theorized that the oil recovery rate can be improve if the solvent is injected in vapour phase to increase the gravitational potential to drain the mobilized oil. Subsequent experimental and modeling studies of Butler and his co-workers (Butler and Mokrys 1991, 1993; Mokrys and Butler 1993; Das and Butler 1994, 1998) and others (Dunn et al. 1989) contributed to the early development of the concept of vapour solvent injection to recover heavy oil and bitumen (VAPEX).

The category of the thermal-solvent assisted gravity drainage processes are the enhanced recovery methods which rely on the gravity to drain the mobilized oil by heat and/or dilution toward the production well. Different gravity drainage recovery processes can be included in this category depending on the range of the injection temperature and the composition of the injection fluid. In the commercially implemented SAGD process, steam is injected to deliver heat and to mobilize bitumen without use of any solvents. Near the final stages of the commercialization are recovery processes such Expanding-Solvent SAGD (ES-SAGD) (Nasr and Isaacs 2001) (also called solvent-assisted SAGD (SA-SAGD) (Dittaro et al. 2013)) in which hydrocarbon solvents are co-injected with steam at temperatures close to the steam temperature to improve the performance of the recovery process by auxiliary in-situ dilution of the bitumen. Experimental and modeling studies (Khaledi et al. 2012, 2015) show that the choice of co-injected solvent affects the complex thermodynamic interaction of steam and solvent, heat transfer, multiphase fluid equilibrium and flow in the porous media and consequently controls the relative enhanced performance of these processes depending the choice of solvent. VAPEX process relies on the injection of vapour hydrocarbon solvent at the reservoir temperature to dissolve in bitumen and mobilize it. It is expected that oil recovery rate by the VAPEX process is considerably lower than thermal steam assisted processes due to limited mass transfer of dissolved solvent in bitumen at reservoir temperature due to the high viscosity of the bitumen. To overcome this limiting mechanism, the heated VAPEX process (Butler and Mokrys 1991 and 1993) utilizes high temperature vapour solvent injection to deliver heat to the in-situ bitumen upon condensation and to dilute the bitumen with the condensed solvent. The result of experimental studies of Butler and Mokrys (1991 and 1993) showed that the heating of solvent in the VAPEX process can enhance the production rate of bitumen several folds. Heating of the injected solvent, condensation and release of heat of vapourization at its saturation point due to temperature difference between the injected vapour and bitumen on vapour-bitumen interface, results in heating and slight viscosity reduction in the bitumen, and forming a drainage bank of condensed solvent on interface, which can significantly improve the dispersive and diffuse mixing of solvent with bitumen that enhances the production rate of the process compared to lower operating temperatures.

ExxonMobil and Imperial Oil have been investigating thermal solvent recovery technologies through an integrated research program that includes fundamental laboratory work, advanced analytical and numerical simulation studies (Dickson et al. 2013a; Khaledi et al. 2015; Mensah-Dartey et al. 2015), laboratory scaled physical modelling (Khaledi et al. 2012) and field piloting (Perlau et al. 2011; Dickson et al. 2013b; Dittaro et al. 2013; Khaledi et al. 2014). This research program is a part of the initiative to develop, improve

and commercialize in-situ recovery technologies (Boone et al. 2011; Boone et al. 2014). Learnings of physical modeling experiments, field pilots and commercialization of three thermal recovery technologies (i.e. SAGD, SA-SAGD, and Liquid Addition to Steam for Enhancing Recovery (LASER) (Leaute 2002; Stark 2013)), are all incorporated into this research program. The program aims at in-depth understanding of process physics and mechanisms, evaluating process performance and behavior, and developing new thermal solvent recovery processes. Recently, the focus of the research program has been to develop High Temperature Multicomponent Solvent Vapour Extraction (HTMS-VAPEX), a variation of the heated VAPEX process using a multi-component solvent such as a commercial diluent, and its enhanced variations such as Azeotropic heated VAPEX process (Khaledi et al. 2013; Khaledi et al. 2014; Boone et al. 2015; Khaledi and Motahhari 2017). In the latter, an optimal fraction of steam is co-injected with vapour solvent to enhance the key performance indicators of the recovery process (Khaledi et al., 2018).

This paper provides a basic overview on the internally developed analytical model for the suite of the thermal solvent gravity drainage processes with applicability to both steam and/or solvent based processes and any combination of them. A detailed review of the related modeling studies is out of the scope of this paper. In general, most of the historically developed models apply either to steam-based processes (Butler et al. 1981; Butler and Stephens 1981; Butler 1985; Butler 1994) or to the isothermal solvent-based processes (Butler and Mokrys 1989; Dunn et al. 1989; Das and Butler 1998). The VAPEX models were developed with the assumption of the concentration-independent diffusion coefficient to analytically solve the second order partial differential equation governing mass transfer. These modes were used to match the laboratory VAPEX experiment results using either concentration-independent (Dunn et al. 1989) or concentration-dependent diffusion coefficients (Butler and Mokrys 1989; Das and Butler 1996, 1998). The latter trials were inconsistent with the basic assumption of the concentration-independent diffusion coefficient to develop the models. Nonetheless, in either of approaches, it was found that diffusion coefficients must be orders-of-magnitude bigger than the reported values to match the model predictions to the lab data. The better than expected performance of the VAPEX process in the lab (in comparison to the model predictions with diffusivity alone) was related (Das and Butler 1998) to several mechanisms occurring in the porous media which were enhancing the mass transfer and were not captured by the models. The simple analytical model of VAPEX incorporating mechanical dispersion as one of these mechanisms was shown to do a better match of the experimental Hell-Shaw cell data (Boustani and Maini 2001).

In this study, a general analytical model for gravity drainage processes is developed by incorporating mass transfer mechanisms (including diffusion and dispersion) and heat transfer mechanism by conduction. In particular, the dependency of diffusion and dispersion coefficients on concentration, fluid and rock properties, and drainage velocities is incorporated. A novel approach is utilized to analytically solve the second order non-linear partial differential equation governing mass transfer within the mass boundary layer. Criteria are defined to isolate the mass transfer boundary layer from the overlaying heat transfer boundary layer whereas their entirety defines the drainage layer. A mathematical expressions is provided to estimate the concentration and temperature variation within the corresponding boundary layers and the contributions of each boundary layer to total flow within the drainage layer. A closed-form analytical model is developed which provides oil drainage rate due to gravity, heat and dilution effects as a function of reservoir and fluid properties.

The applicability of the developed model is demonstrated by analysis of the experimental data of the VAPEX process from literature. It is also shown how the performance of the VAPEX process is enhanced by increasing the pressure and temperature of the injected vapour solvent. The developed model is utilized to investigate the performance of the heated VAPEX process in the field.

Model Development

Definitions

In the thermal-solvent assisted gravity drainage recovery processes, the mobilized bitumen drains toward the production well by the gravitational forces. In the mobile bitumen layer, the viscosity of the native bitumen is reduced due to temperature increase and dilution with light hydrocarbon compounds of the injected solvent. Figure 1(a) shows a schematic cross sectional view of the vapour chamber in these processes. The most important period representing the steady state rate performance in gravity drainage processes is the lateral growth of the chamber. Therefore, in the presented study the focus has been on modeling of the lateral growth of the chamber. In the schematic view of Figure 1, the chamber is growing laterally and its upward growth is stopped due to the impermeable overlaying layers. Figure 1(b) abstractly illustrates how the temperature and concentration of the solvent vary in front of the advancing bitumen-vapour interface in an infinitesimal segment of the drainage layer in y-direction. In general, it is expected that two boundary layers exist within the drainage layer due to different time scales of heat and mass transfer mechanisms. In the mass boundary layer, denoted by Ξ_C, the concentration of the solvent varies with distance from the interface from a maximum value (C_o) to a defined cut-off value ($C_{\xi C}$). Within this boundary layer, the mobilized oil has reduced viscosity due to combined effects of heat and dilution. Solvent content below defined cut-off concentration has no material effect on the viscosity of solvent and bitumen mixture. In the heat boundary layer, denoted by Ξ_T, the temperature varies from a maximum value (T_o) to the initial temperature of the reservoir (T_i). Theoretically, the heat boundary layer encompasses the mass boundary layer as well. However, for this modeling study, we strictly isolate and de-couple these two boundary layers to have fully analytical solutions for the mass and heat transfer mechanisms. By definition, the heat boundary layer starts from the distance ξ_C in front of the advancing front in which the solvent concentration is equal to the cut-off concentration value. This decoupling method and simplifying assumptions are valid as ξ_C is order of magnitudes smaller than the heat transfer boundary layer thickness. Figure 1(c) is a magnification of the temperature, concentration and bitumen drainage velocity variations with the mass boundary layer. Given the order of magnitude difference between the thicknesses of Ξ_C and Ξ_T, it is expected that the temperature variation within temperature boundary layer to be small. The demonstrated bitumen drainage velocity profile is arbitrary for illustrative purposes as its exact shape strongly depends on concentration and temperature profiles and the absolute values of the boundary values.

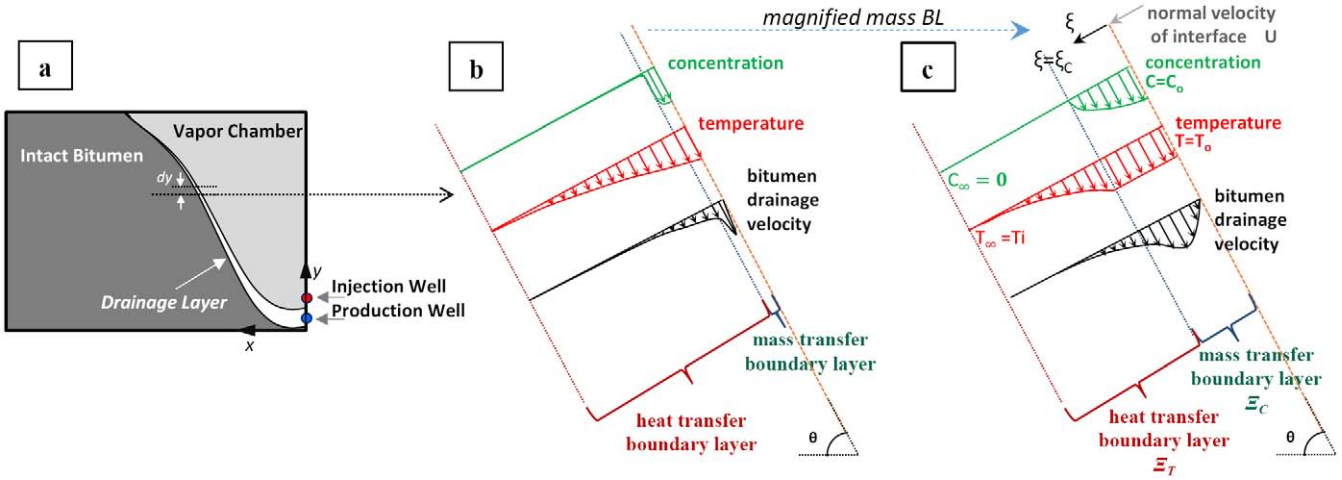

Figure 1—a) Thermal-Solvent Gravity Drainage Schematics; b) Cross section of the drainage layer; c) Cross section of the drainage layer with magnified mass transfer boundary layer.

Unless otherwise stated, the overarching assumptions in all subsequent sections are:

- The advancing bitumen-vapour front is defined as a sharp gas/liquid interface. The oil saturation behind the interface equals to residual oil saturation.
- The concentration and temperature distributions ahead of advancing front are steady state profiles and do not change with time.
- The recovery process is isobaric (constant pressure) operation; hence, the temperature and concentration at interface are determined by thermodynamic equilibrium between the gas and liquid phase at a šgiven pressure.
- The solvent and bitumen are single component hydrocarbons; hence, no heavy phase precipitates and deposits upon mixing of solvent and bitumen.
- There is no volume change (shrinkage or expansion) upon mixing of solvent and bitumen.
- The heat transfer is governed by conduction. The mass transfer mechanism is governed by composition and temperature dependent diffusion and velocity-dependent mechanical dispersion in porous media.

Temperature Distribution

We follow Butler's approach (1981) to develop the temperature distribution function ahead of the advancing front since all the assumptions are equivalent to his work. Fourier's second law governs the one-dimensional transient heat conduction ahead of the advancing front as:

$$\frac{\partial}{\partial x}\left(\alpha_T \frac{\partial T}{\partial x}\right) = \frac{\partial T}{\partial t} \qquad \text{Equation 1}$$

The above equation for each segment on the interface is transferred to a new reference frame moving with the advancing front as:

$$\frac{\partial^2 T}{\partial \xi^2} + \frac{U}{\alpha_T}.\frac{\partial T}{\partial \xi} = \frac{1}{\alpha_T}.\frac{\partial T}{\partial t} \qquad \text{Equation 2}$$

In the above formulation, it is assumed that fluid properties (density, heat capacity, and thermal conductivity) are independent of temperature and composition; hence, α_T is constant. ξ is the distance from the front and is defined by velocity of the advancing front at the corresponding segment (U) as:

$$\xi = x - \int_0^t U.dt \qquad \text{Equation 3}$$

Assuming steady state temperature profile, equation 2 reduces to:

$$\frac{\partial^2 T}{\partial \xi^2} + \frac{U}{\alpha_T}.\frac{\partial T}{\partial \xi} = 0 \qquad \text{Equation 4}$$

with following boundaries condition according to the definition of the heat boundary layer:

$$T = T_o \quad @\ \xi = 0 \qquad \text{Equation 5}$$

$$T = T_i \quad @\ \xi = \infty \qquad \text{Equation 6}$$

where T_o is the temperature at the interface and T_i is the initial bitumen reservoir temperature. The analytical solution of the equation 4 with the boundary conditions of 5 and 6 is:

$$T = T_i + (T_o - T_i).\exp\left(\frac{-U.\xi}{\alpha_T}\right) \qquad \text{Equation 7}$$

Concentration Distribution

The mass transfer ahead of advancing front is governed by one-dimensional Fick's second law as:

$$\frac{\partial}{\partial x}\left(K_D \frac{\partial C}{\partial x}\right) = \frac{\partial C}{\partial t} \quad \text{Equation 8}$$

where C is the solvent concentration (volume fraction), and K_D is the total mass transfer coefficient equal to sum of composition-dependent diffusion and velocity-dependent mechanical dispersion in porous media as is shown later with equation 17. In this study, we will show that the total mass transfer coefficient in the thermal-solvent assisted gravity drainage recovery process can be assumed as a direct function of solvent concentration. Hence, the equation 8 is transferred to the moving reference frame defined by equation 3 as:

$$\frac{\partial^2 C}{\partial \xi^2} + \frac{1}{K_D}.\frac{\partial K_D}{\partial C}.\left(\frac{\partial C}{\partial \xi}\right)^2 + \frac{U}{K_D}.\frac{\partial C}{\partial \xi} = \frac{1}{K_D}.\frac{\partial C}{\partial t} \quad \text{Equation 9}$$

Assuming steady state concentration profile, equation 9 reduces to:

$$\frac{\partial^2 C}{\partial \xi^2} + \frac{1}{K_D}.\frac{\partial K_D}{\partial C}.\left(\frac{\partial C}{\partial \xi}\right)^2 + \frac{U}{K_D}.\frac{\partial C}{\partial \xi} = 0 \quad \text{Equation 10}$$

with following boundary condition according to the definition of the mass boundary layer:

$$C = C_o \quad @\ \xi = 0 \quad \text{Equation 11}$$

$$C = 0 \quad @\ \xi = \infty \quad \text{Equation 12}$$

where C_o is the solvent concentration at the interface.

Equation 10 is a 2nd-order non-linear PDE without a general analytical solution. However, an analytical solution can be developed if the dependency of K_D to the concentration is expressed in the form of an "*n-th*" order polynomial function as follows:

$$K_D = \sum_{i=0}^{n} \kappa_i . C^i \quad \text{Equation 13}$$

Replacing equation 13 in equation 10, we develop the following fully analytical solution of the non-linear PDE of equation 10 with the boundary conditions of 11 and 12:

$$\xi = -\left(\frac{\kappa_0}{U} ln\left(\frac{C}{C_o}\right) + \frac{1}{U}.\sum_{i=1}^{n} \frac{\kappa_i}{i}\left(C^i - {C_o}^i\right)\right) \quad \text{Equation 14}$$

Without loss of the generality of the approach, in this study, we use a "*3rd*" order polynomial expression for the concentration dependency of K_D in equation 13 as shown in the next section; hence, the equation 14 is re-written, for this special case, as:

$$\xi = -\left(\frac{\kappa_0}{U} ln\left(\frac{C}{C_o}\right) + \frac{1}{U}.\sum_{i=1}^{3} \frac{\kappa_i}{i}\left(C^i - {C_o}^i\right)\right) \quad \text{Equation 15}$$

Assuming no concentration-dependency of the total mass transfer coefficient ($K_D = \kappa_0$), the equation 14 reduces to the following concentration distribution function analogous to the temperature distribution function of equation 7:

$$C = C_o . \exp\left(\frac{-U.\xi}{\kappa_0}\right) \quad \text{Equation 16}$$

where κ_0 is the mutual diffusion coefficient of the solvent and bitumen system. Equation 16 is the special solution of equation 8 with simplifying assumption of no concentration and velocity dependency for the mass transfer coefficient, that has been used by other authors as described in the introduction. The solution of this equation with concentration, temperature, and velocity dependency in this work is described in the next section.

Mass Transfer Coefficient

Assuming the infinitesimal segment of the drainage boundary layer in the thermal-solvent assisted gravity drainage processes, the one-dimensional mass transfer occurs in ξ-direction which is perpendicular to drainage velocity streamlines. Hence, the 1-D mass transfer coefficient due to diffusion and dispersion can be expressed as:

$$K_D = \frac{D_{SB}}{\tau} + a_C \frac{V_{d\,l}}{\phi . S_l} \qquad \text{Equation 17}$$

where D_{SB} is the mutual diffusion coefficient of the solvent and bitumen system; τ, α_C, φ are all properties of the porous media; namely, tortuosity, transverse dispersivity and porosity, respectively. S_l and $V_{d\,l}$ are the saturation and Darcy velocity (in the direction perpendicular to ξ) of the liquid hydrocarbon phase, respectively. Note that in developing equation 17, we neglect the longitudinal dispersion due to the velocity of the advancing front in the perpendicular direction to drainage velocity streamlines as this velocity is much smaller than the drainage velocities. In the thermal-solvent assisted gravity drainage processes, $V_{d\,l}$ is equal to the liquid drainage velocity tangent to the local curvature of the vapour-liquid interface. Given the temperature and concentration change within the drainage layer, the diffusion and dispersion (due to change in drainage velocity) and consequently total mass transfer coefficient change by the distance from the interface, ξ.

Equation 18 relates (Butler and Mokrys 1989) the mutual diffusion coefficient (D_{SB}) of a binary mixture of solvent and bitumen to the intrinsic diffusion coefficients of the components in the mixture (D_S and D_B for solvent and bitumen, respectively);

$$D_{SB} = D_S . (1 - C) + D_B . C \qquad \text{Equation 18}$$

This equation is generally applicable to: 1) a mixture without volume change upon mixing in static diffusion conditions; or 2) where the volume change is compensated by flow in transverse direction to the diffusion. The latter is the case for the steam-solvent assisted gravity drainage recovery process. In addition to the explicit dependency of the mutual diffusion coefficient to the concentration by equation 18, D_S and D_B are also generally functions of the concentration-dependent mixture properties.

In this study, without loss of generality of the approach, we use Wilke and Chang's (1955) correlation to estimate the intrinsic diffusion coefficients of the bitumen and solvent components in their binary mixtures at any given concentration and temperature. Considering the assumption of constant temperature within the mass transfer boundary layer which was discussed previously, the diffusion coefficient becomes a function of concentration only at a constant temperature within the mass transfer boundary layer. Figure 2(a) shows how the intrinsic diffusion coefficients of the bitumen and n-pentane in their binary mixtures change with concentration. The mutual diffusion coefficient of n-pentane and bitumen is calculated by equation 18 and is shown as the dashed line. D_{SB} is equal to the intrinsic diffusion coefficient of n-pentane in an infinitely dilute solution of n-pentane in bitumen when the n-pentane volume fraction is equal to 0. Similarly, the mutual diffusion coefficient of an infinitely dilute solution of bitumen in n-pentane mixture is equal to the intrinsic diffusivity of bitumen in pure n-pentane.

In order to satisfy the requirement of equation 13, the functionality of the mutual diffusion coefficient to the concentration must be expressed in the form of an "*n-th*" order polynomial. In this study, without loss

of the generality of the approach, we use a second order polynomial to fit the functionality of the estimated mutual diffusivity values to the concentration in the following form:

$$D_{SB} = D_{S\infty} + (D_{B\infty} - D_{S\infty}).C^2 \quad \text{Equation 19}$$

Figure 2(b) shows the quality of the fit of the 2nd order polynomial expressions to the estimated mutual diffusivity values of the n-pentane and bitumen mixtures at two different temperature conditions.

For thermal-solvent assisted gravity drainage processes, according to Darcy's law, the drainage velocity of the liquid hydrocarbon phase (i.e. mixture of solvent and bitumen) at a segment of interface and at any distance from the interface ξ is given by (Butler et al. 1981):

$$V_{d\,l} = k_{e\,l}.g.\,sin(\theta).\left(\frac{\rho_l - \rho_g}{\mu_l}\right)_{T,P,C} \quad \text{Equation 20}$$

where $k_{e\,l}$ is the effective permeability to liquid HC phase, g is the gravitational constant, and θ is the angle of the tangent to the interface at the given segment with the horizon. ρ_l and ρ_g are densities of the liquid HC and gas phase, respectively. μ_l is the viscosity of the liquid HC phase. In general, these fluid properties depend on temperature, pressure and concentration. Note that, in this study and for the sake of completeness, we do not neglect the density of the vapour phase in comparison to the liquid phase as the density of vapour hydrocarbons is comparable to liquid phase as the pressure and temperature approaches the critical conditions of the injected fluid. However, in general, the critical conditions are not approached in the gravity drainage processes of this study.

Assuming the pressure of the vapour chamber is constant, the temperature of the gas phase is also constant, which is determined by the thermodynamic equilibrium between the gas phase and residual liquid phase within the depleted chamber. The temperature of the oil phase changes with distance from the interface within the mass boundary layer. Given the order of magnitude difference between the thickness of the mass boundary layer and heat boundary layer, the temperature variation within the mass boundary layer is small in comparison to the temperature change within the heat boundary layer. In order to satisfy the requirement of equation 13, we estimate the oil phase properties at the fixed temperature of the interface (T_o) which is equal to the temperature of gas phase. Hence, the fluid properties in equation 20 only depend on the concentration at the constant temperature of T_o as follows:

$$V_{d\,l} = k_{e\,l}.g.\,sin(\theta).\left(\frac{\Delta\rho_{l-g}}{\mu_l}\right)_{C,To} \quad \text{Equation 21}$$

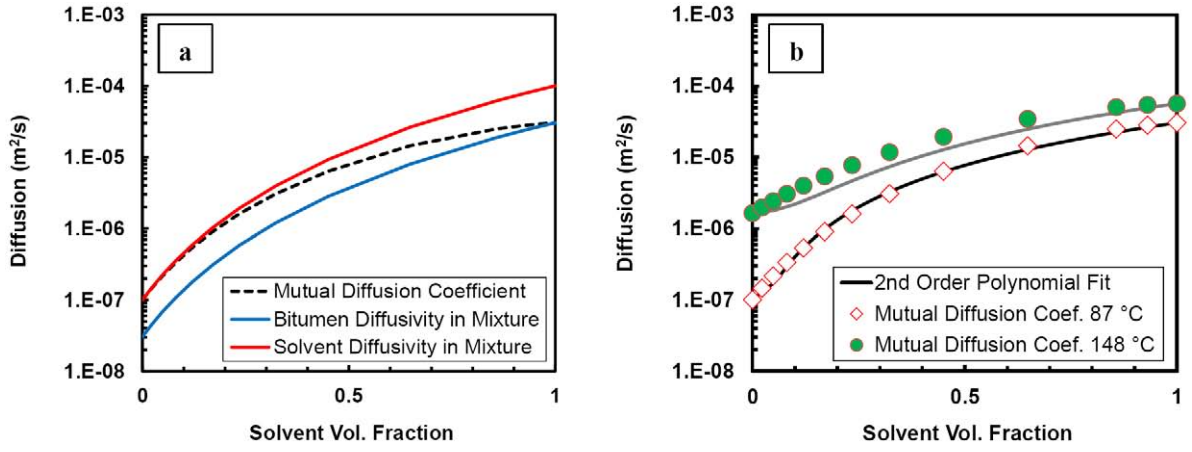

Figure 2—a) The concentration dependency of the intrinsic diffusivities of n-C5 and bitumen in their mixture and the resulted mutual diffusion coefficient at 87 °C; b) 2nd order polynomial representation of mutual diffusion coefficient of n-C5 and bitumen in their mixture at 87 and 148 °C.

where $\Delta\rho_{l-g}$ is the difference between the densities of liquid hydrocarbon phase (concentration dependent) and the corresponding vapour phase in equilibrium. In this study, without loss of the generality of the approach, we use a third order polynomial to fit the functionality of the fluid properties to the concentration in the following form:

$$\left(\frac{\Delta\rho_{l-g}}{\mu_l}\right)_{C,To} = \chi_0 + \chi_1.C + \chi_2.C^2 + \chi_3.C^3 \quad \text{Equation 22}$$

Figure 3 shows the quality of the fit of the 3nd order polynomial expressions to the estimated fluid properties of the n-pentane and bitumen mixtures at two different temperature conditions. In this figure, the symbols denote the estimated fluid properties using non-linear mixing rules which are verified against available experimental density and viscosity data of the n-pentane and bitumen mixtures with varying compositions. Note that the effect of the formation of the heavy phase due to asphaltenes precipitation is not included in the estimated fluid properties.

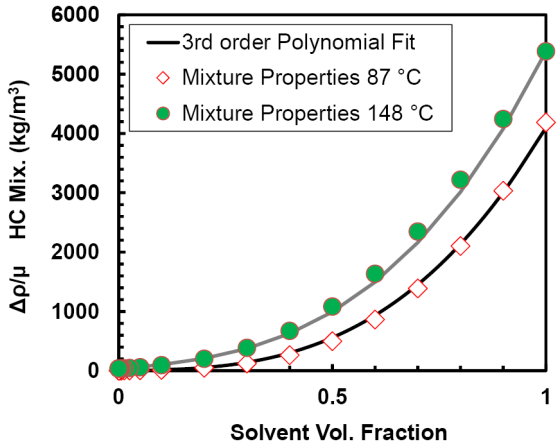

Figure 3—3rd order polynomial representation of the fluid properties of n-C5 and bitumen mixtures at 87 and 148 °C.

Using the polynomial expressions of equations 19 and 22 for the diffusivity and the fluid properties of the solvent and bitumen mixtures, the total mass transfer coefficient (equation 17) can be written in the form of a 3rd order polynomial as follows:

$$K_D = \kappa_0 + \kappa_1.C + \kappa_2.C^2 + \kappa_3.C^3 \quad \text{Equation 23}$$

where:

$$\kappa_0 = \frac{D_{S\infty}}{\tau} + k_{el}.g.\ sin(\theta).\chi_0 \quad \text{Equation 24}$$

$$\kappa_1 = k_{el}.g.\ sin(\theta).\chi_1 \quad \text{Equation 25}$$

$$\kappa_2 = \frac{(D_{B\infty} - D_{S\infty})}{\tau} + k_{el}.g.\ sin(\theta).\chi_2 \quad \text{Equation 26}$$

$$\kappa_3 = k_{el}.g.\ sin(\theta).\chi_3 \quad \text{Equation 27}$$

Flow in Drainage Layer

The total bitumen flow rate within the drainage boundary layer for an element of unit width at each segment of interface (see Figure 1) can be calculated by integrating the flow rate parallel to the interface at each distance ξ from the interface as:

$$q_{oil} = \int_0^{\infty} V_{d\,l} \,.\, (1 - C)\, d\xi \qquad \text{Equation 28}$$

The factor *(1-C)* accounts for the volume fraction of the solvent in the draining hydrocarbon liquid phase. Replacing the relationship for the drainage velocity in the above equation, the oil flow rate is:

$$q_{oil} = k_{e\,l} \,.\, g.\, sin(\theta) \left[\int_0^{\xi_C} \left(\frac{\Delta\rho_{l-g}}{\mu_l} \right)_{C,To} .(1 - C).\, d\xi + \int_{\xi_C}^{\infty} \left(\frac{\Delta\rho_{l-g}}{\mu_l} \right)_{T} .\, d\xi \right] \qquad \text{Equation 29}$$

Where ξ_C is the thickness of the mass boundary layer at the given segment of the interface. In the above equation, it is assumed that the effective permeability to the liquid hydrocarbon phase is the same within the mass and heat boundary layers. The first and the last integral in the above equation is accounting for the drainage of the oil within the mass and heat boundary layers, respectively.

The dependence of the temperature and concentration to distance from the interface is given by the general relationships of equations 7 and 15 (for 3rd order polynomial expression of the concentration dependency of the total mass transfer coefficient), respectively. Using these relationships, we change the variable of integration from distance to the concentration and temperature for the first and the last integrals, respectively; as below:

$$q_{oil} = \frac{k_{e\,l} \,.\, g.\, sin(\theta)}{U} (I_T + I_C) \qquad \text{Equation 30}$$

where:

$$I_C = \int_{C_{\xi_C}}^{C_0} \left(\frac{\Delta\rho_{l-g}}{\mu_l} \right)_{C,To} .(1 - C).\, \left(\frac{\kappa_0}{C} + \kappa_1 + \kappa_2 . C + \kappa_3 . C^2 \right) . dC \qquad \text{Equation 31}$$

$$I_T = \int_{T_i}^{T_{\xi_C}} \left(\frac{\Delta\rho_{l-g}}{\mu_l} \right)_{T} . \frac{\alpha_T}{T - T_i} dT \qquad \text{Equation 32}$$

where $C_{\xi C}$ is the cut-off concentration of the mass boundary layer. The distance from the interface to reach cut-off concentration is estimated by replacing $C_{\xi C}$ in equation 15. $T_{\xi C}$ is the temperature at the mass transfer boundary layer cut-off distance and can be estimated by replacing ξ_C in equation 7.

We integrate equation 31 with replacing the 3rd order polynomial expression for the dependency of fluid properties to concentration at the interface temperature of T_o (equation 22) resulting in:

$$I_C = \gamma_0\, ln\left(\frac{C_o}{C_{\xi_C}} \right) + \sum_{k=1}^{7} \frac{\gamma_k}{k} \left({C_o}^k - {C_{\xi_C}}^k \right) \qquad \text{Equation 33}$$

where coefficients γ_k (k=0…7) are functions of coefficients κ_i (i=0…3) and χ_j (j=0…3) with detailed dependencies given in Appendix A.

Following the approach by Butler et al. (1981), we model the temperature-dependency of the fluid properties to temperature within the heat boundary layer as:

$$\left(\frac{\Delta\rho_{l-g}}{\mu_l} \right)_T = \left(\frac{\Delta\rho_{l-g}}{\mu_l} \right)_{T_{ref}} . \left(\frac{T - T_i}{T_{ref} - T_i} \right)^m \qquad \text{Equation 34}$$

where T_{ref} is the reference temperature at which the reference fluid properties are assessed. It is worthwhile to note that:

$$\left(\frac{\Delta\rho_{l-g}}{\mu_l}\right)_T = \frac{\rho_{l\,(T)} - \rho_{g\,(To)}}{\mu_{l(T)}} \quad \text{Equation 35}$$

where $\rho_{l\,(T)}$ and $\mu_{l(T)}$ are the bitumen density and viscosity at temperature T and $\rho_{g\,(To)}$ is the density of the vapour at the fixed temperature of T_o.

We integrate equation 32 with replacing equation 34 for the dependency of fluid properties to temperature resulting in:

$$I_T = \frac{\alpha_T}{m}.\left(\frac{\Delta\rho_{l-g}}{\mu_l}\right)_{T_{ref}}.\left(\frac{T_o - T_i}{T_{ref} - T_i}\right)^m.\left[exp\left(\frac{-\alpha_{\xi_C}}{\alpha_T}\right)\right]^m \quad \text{Equation 36}$$

where $\alpha_{\xi C}$ is defined by the following equations based on the definition of distance from the interface to reach cut-off concentration:

$$\alpha_{\xi_C} = U.\xi_C \quad \text{Equation 37}$$

$$\alpha_{\xi_C} = -\left(\kappa_0.ln\left(\frac{C_{\xi_C}}{C_o}\right) + \sum_{i=1}^{3}\frac{\kappa_i}{i}\left({C_{\xi_C}}^i - {C_o}^i\right)\right) \quad \text{Equation 38}$$

Since the flow of the mobilized bitumen within the mass boundary layer ($T_{\xi_C} < T < T_o$) due to the heat and temperature increase is accounted for in I_C, the parameter α_{ξ_C} reduces the I_T by the appropriate fraction to account for it. If no solvent is injected in the recovery process (SAGD), C_o and C_{ξ_C} are equal to 0 (no mass boundary layer; $\alpha_{\xi_C} = 0$), equation 30 reduces to the equation developed by Butler et al. (1981) for SAGD process ($T_{ref} = T_o$):

$$q_{oil} = \frac{k_{e\,l}.g.\,sin(\theta).\alpha_T}{m.U.\left(\frac{\mu_l}{\Delta\rho_{l-g}}\right)_{T_o}} \quad \text{Equation 39}$$

Total Oil Production Rate

We follow Butler and his co-workers' approach (Butler et al. 1981, Butler and Mokrys 1989) to estimate the total oil production rate by the thermal-solvent assisted gravity drainage process. Details of their approach can be found elsewhere. In this approach, the movement of the interface at each segment is related to the material balance within the corresponding segment of the drainage layer. In addition, it is assumed that the drainage layers are continually attached to the production well (TANDRAIN assumption by Butler and Stephens (1981)). Hence, we calculate the total oil production rate by the following closed form equation:

$$Q = 2L\sqrt{1.5\,\phi\,\Delta S_l(I_T + I_C)\;k_{r\,l}\,g\,H} \quad \text{Equation 40}$$

where L is the length of the well, H is the total reservoir pay height and ΔS_l is the difference between the initial and residual bitumen saturation. If no solvent is injected in the recovery process (SAGD), I_C is equal to 0 and, equation 40 reduces to the equation developed by Butler and Stephens (1981) for the SAGD process ($T_{ref} = T_o$):

$$Q = 2L\sqrt{\frac{1.5\,\phi\,\Delta S_l\alpha_T\,k_{r\,l}\,g\,H}{m.\left(\frac{\mu_l}{\Delta\rho_{l-g}}\right)_{T_o}}} \quad \text{Equation 41}$$

In the original theory of Butler et al. (1981), the coefficient is 2 instead of 1.5. To calculate the front advance velocity at any depth y ($h_{tan} < h < H$ where $h_{tan} = 2H/3$ for TANDRAIN assumption), equation 40 with the coefficient of 2 instead of 1.5 must be used.

It is worthwhile to note that, in general, the contribution of the mass boundary layer (I_C) to the flow within the drainage layer has a secondary dependency to θ as the total mass transfer coefficient varies with θ by equations 24 to 27. Hence, it is not mathematically feasible to develop a closed form solution for the total oil production rate without any simplifications. In this study, we evaluate I_C in equation 30 at θ = 45° representing an average total mass transfer coefficient over the length of the drainage interface. A sophisticated estimation of the total production rate can be achieved using a semi-analytical sequential approach (Butler 1985) by dividing the reservoir height to small segments and tracking the location and inclination angle of the interface and consequently calculations of I_T and I_C for each segment over small time-steps.

In addition, in this study, we assume that that the effective permeability to liquid hydrocarbon phase is the same within the mass and heat boundary layers. Our analysis including laboratory and numerical simulation studies (using very fine-grid simulation models in lab and field scale) indicate that this assumption is not valid for all applications of steam and solvent in the gravity drainage processes. One can determine the saturation and relative permeability of the liquid hydrocarbon and water in each boundary layer by estimating their fractional flow and using the physical and transport properties of the draining liquids. However, the inclusion of this complexity in the modeling approach is out of the scope of this study.

Results and Discussion

We validate the developed model and demonstrate its applicability using a full dataset of 15 VAPEX experiments (Yazdani and Maini 2005, 2006) conducted at close to ambient temperature conditions using Butane as the injected solvent. The height of the physical model and the particle size of the porous media was varied in different experiments to investigate the effect of pay height and permeability on the process performance. Table 1 and 2 summarizes the details of the VAPEX experiments. Different heavy oil samples with similar physical and transport properties at the test temperature were used to saturate the physical models. Since, all the required phase behavior data is not available for all of the oil samples, we use the experimental PVT and viscosity data of Frog Lake oil and Butane mixtures (Yazdani and Maini 2010) to provide the required inputs to the model (including Butane solubility in the heavy oil, and variation of density of viscosity of mixture with the concentration). Note that we assume no 2nd liquid phase is being formed in these experiments despite the proximity of the ~0.4 volume fraction solubility of Butane in the heavy oil at the test temperature and pressure to the onset of the formation of the 2nd heavy hydrocarbon phase.

In addition, we utilize the model to demonstrate the mechanisms of the enhanced mass transfer by the formation of the condensed solvent drainage layer in front of the advancing front in the heated VAPEX process. Last, we study the performance of the heated VAPEX process in a typical Athabasca oilsands reservoir with pay height of 18m, porosity of 0.33 and permeability of 2.4 D, initial oil saturation of 0.73 and average grain diameter of 0.2 mm. The bitumen properties are generic to the Athabasca area with a density of 1017 kg/m^3 and a viscosity of 4×10^6 mPa.s at reservoir condition (7 °C).

Note that we do not validate the model for the thermal-only gravity drainage processes as several other studies (including Butler and Stephens 1981) confirmed the applicability of the TANDRAIN approach.

Table 1—Name, description and dimensions of the Physical Models used for the VAPEX experiments (Yazdani and Maini 2005, 2006).

Description	Rectangular			Cylindrical	
Model Name	R#1	R#2	R#3	C#2	C#3
Height (cm)	7.5	15	30	60.1	100.5
Width (cm)	11.3	22.5	45	84.6	148.2
Depth (m)	2.5	2.5	2.5	3.2	2.6

Table 2—Characteristics of the porous media in the VAPEX experiments (Yazdani and Maini 2005, 2006).

US Mesh Size	Saturation	Porosity	Permeability (D)
12–16 Glass bead	0.047	0.365	640
16–20 Glass bead	0.071	0.368	330
20–30 Sand	0.09	0.341	220

Model Validation

We validate the model by matching the estimated oil production rate to the measured value of the experiment using Model-C#3 with 12-16 US mesh size glass beads. The dispersivity of the medium was used as the tuning parameter and the best match was resulted by using $a_C = 1.62 \times 10^{-5}$ m. We assess the properties of the drainage layer at a segment of the interface at $y = 2H/3$ when the local inclination angle of the interface is equal to 45°. The results are depicted in Figures 4 and 5. Since the VAPEX process in this experiment is isothermal, there is no heat transfer BL and the thickness of the mass transfer BL is ~4 mm. Figure 4(a) shows how the concentration of the solvent changes within the mass transfer BL in front of the advancing front. In general, the concentration change is gradual (0.46 to 0.2 vol. fr. within the first 90% of the BL thickness), with an abrupt drop to 0 at the last 10% of the mass transfer boundary layer. This shape of the concentration profile may be interpreted as the concentration shock (Oballa and Butler 1989, Nenninger and Dunn 2008, Okazawa 2009) in a macro-scale observation and is mainly due to concentration dependency of the total mass transfer coefficient as shown in Figure 5(a). The total mass transfer coefficient is virtually equal to the dispersion coefficient as the latter is approximately 2 orders of magnitude larger than the diffusion coefficient. Figure 5(b) demonstrates the concentration dependency of the diffusion and velocity-dependent dispersion coefficients at the test temperature and porous media conditions. Both of these mass transfer coefficients change by 2-3 orders of magnitude as the concentration of the solvent drops from 0.2 to 0. Hence, the transport properties of the solvent and bitumen mixture (namely viscosity and diffusion) act as the restrictive factors to suddenly limit the mass transfer of the solvent into the bitumen and to drop its concentration to 0. It is worthwhile to note that, in this segment of the drainage boundary layer, the liquid hydrocarbon drainage velocities vary almost linearly with distance from the interface as shown in Figure 4(b). The heavy oil drainage velocity follows the same linear trend within the first 90% of the BL thickness. However, it merges to the drainage velocity of the total liquid hydrocarbon phase at $0.0036 \text{ m} < \xi < \xi_C$ as the drainage layer becomes leaner in the butane content.

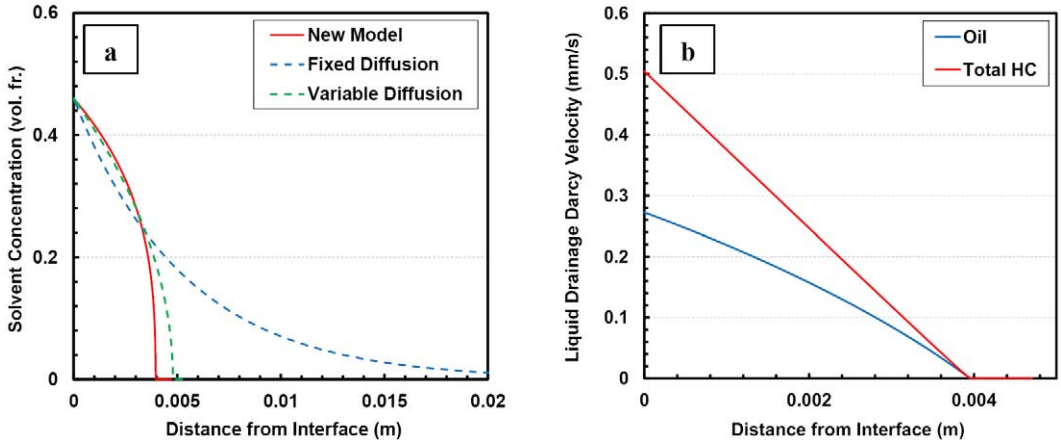

Figure 4—a) Concentration profile within the mass transfer boundary layer predicted by the new model and including dispersion and variable diffusivity, or fixed diffusivity, or variable diffusivity; b) Predicted drainage velocities by the new model.

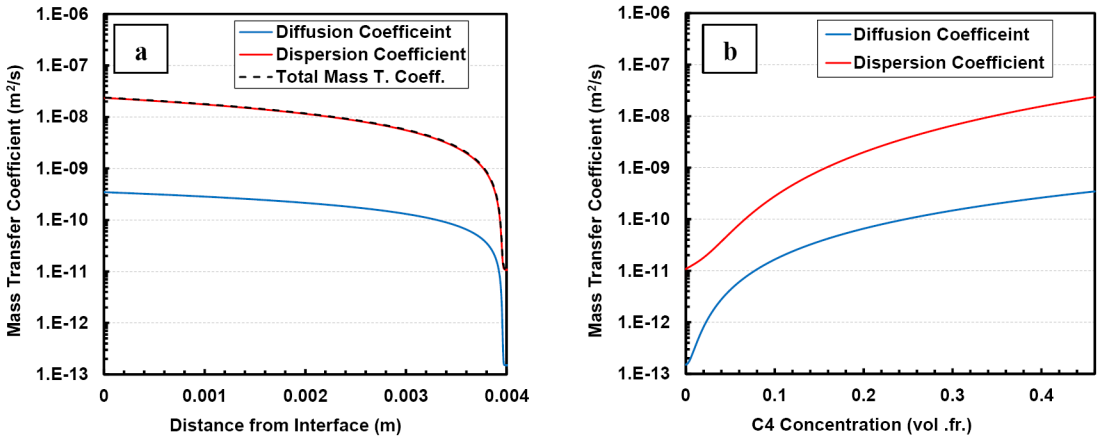

Figure 5—a) Mass Transfer coefficients within the mass transfer boundary layer predicted by the new model; b) Concentration-dependency of the diffusion and velocity-dependent dispersion coefficients at the test temperature and porous media conditions.

Figure 4(a) also demonstrates how the concentration changes within the mass transfer boundary layer for the two other modeling approaches of constant diffusion and variable diffusion with no dispersion. In both approaches, we matched the experimental oil production rate with the model (equation 40) without including dispersion ($a_C = 0$) and using: 1) concentration-independent diffusion coefficient (constant D_{SB}); or 2) concentration-dependent diffusion coefficient (constant $D_{S\infty}$ and $D_{B\infty}$) by equation 19. As reported in Table 3, in both approaches, the adjusted values of the diffusion coefficients are almost 1-2 orders of magnitude greater than the actual diffusion coefficients. In fact, these inflated values of the diffusion coefficients compensate for the exclusion of the dispersive mixing mechanism in the models (Boustani and Maini 2001). Despite having a slightly wider mass transfer boundary layer in approach 2, the form of the concentration profile agrees with the concentration shock observation when both variable diffusion and dispersive mixing are considered. In contrast, the mass transfer boundary layer thickness is almost ~0.03 m in approach 1 as the concentration decreases in a gradual exponential form with the distance from the interface. The concentration variation highlights the importance of the modeling approach and consideration of viability and dependency of the mass transfer coefficient to fluid and flow properties.

Table 3—The numerical values of mass transfer parameters to match the VAPEX experimental data using butane and Model-C#3 with 12-16 US mesh size glass beads.

Mass Transfer Parameters	New Model	Fixed Diffusion	Variable Diffusion
$D_{S\infty}$ (m²/s)	1.64×10^{-9}	–	1.31×10^{-7}
$D_{B\infty}$ (m²/s)	1.51×10^{-13}	–	1.21×10^{-11}
D_{SB} (m²/s)	Equation 19	1.55×10^{-8}	Equation 19
Dispersivity (m)	1.62×10^{-5}	0	0

Scale-Dependency of Dispersion in Random Packs

We evaluate the applicability of the developed model against the full data set of the VAPEX experiments. First, we use the acquired dispersivity values from matching the experiment using Model-C#3 with 12-16 US mesh size glass beads to predict the oil production rate of the experiment using Model-C#3 with 16-20 and 20-30 US mesh size glass beads. As shown in Figure 6, the model under-predicts the oil production rates by 25-35%.

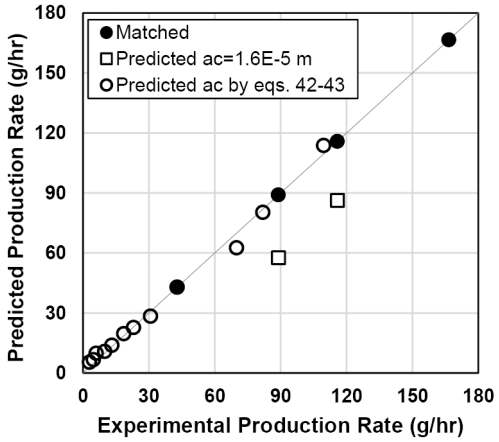

Figure 6—The estimated oil production rate of VAPEX experiments versus the reported experimental values by Yazdani and Maini (2005, 2006); open squares are predicted using dispersivity of Model-C#3 with 12-16 glass beads and open circles are predicted using the developed functionalities of dispersivity with glass beads size and scale of the mass transfer zone.

Perkins and Johnston (1963) report that the dispersivity for a random pack of beads is proportional to the average diameter of the beads (d_P) as follows:

$$a_C \propto \sigma . d_P \qquad \text{Equation 42}$$

where σ is a measure of inhomogeneity of the pack depending on multiple factors including shape, size and size distribution of the beads, and permeability heterogeneities which can be substantial as the scale of the mixing zone becomes greater (Gelhar et al. 1992, Zheng and Bennett 1995). Hence, we determine the dispersivity of the Model-C#3 packed with 16-20 and 20-30 US mesh size glass beads by matching the oil production rates predicted by the model to the experimental values. Figure 7(a) shows how the dispersivity changes with the average glass bead diameter of each pack. Despite the lower oil production rates in these experiments in comparison to the previous experiment in higher permeability medium, larger dispersivity values are required to match the experimental data. Consequently, the drainage interface advances slower and the solvent penetration and loading in front of the interface is greater as shown in Figure 7(b). The observed overall trends in Figure 7(a) are in agreement with Perkins and Johnston (1963) interpretation of the available dispersivity data. The smaller the glass beads size, the less homogenous is the packing and the greater the dispersivity of the porous medium.

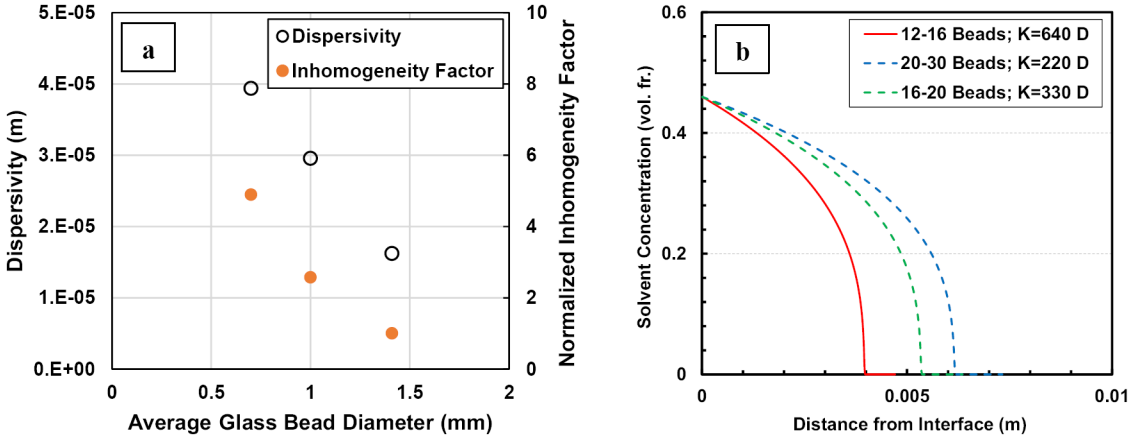

Figure 7—a) Functionality of the dispersivity and inhomogeneity factor (normalized wrt. the value for 12-16 glass bead pack) of models C#3 with the average glass beads size of the pack; b) Predicted concentration profile within the mass transfer boundary layer for VAPEX experiments in Model-C#3 using different glass bead packs.

To investigate the dependency of the dispersivity to the size and scale of the mass transfer zone, we match the estimated oil production rate by the model prediction to the reported experimental value of model R#3 with 12-16 US mesh size glass beads as indicated on Figure 6. The adjusted dispersivity value for this experiment is 3.7×10^{-6} m in comparison to 1.6×10^{-5} m using models C#3 and R#3 with similar glass beads size, respectively. We use the estimated thickness of the mass transfer boundary layer ($\xi_{C\,diff}$) by the model (assuming only diffusion is the driving force) to develop the following scale-dependency of the inhomogeneity factor (σ) of the dispersivity for any given experiment:

$$\frac{\sigma}{\sigma_o} = \left(\frac{\xi_{C\ \ diff}}{\xi_{C\ \ diff_o}}\right)^{2.5} \qquad \text{Equation 43}$$

where σ_o and $\xi_{C\,diff_o}$ are the inhomogeneity factor and the estimated thickness of the mass transfer boundary layer (diffusion only) for the reference experimental porous media. The exponent 2.5 is found to provide the best correlation between the matched dispersivities of the experiments using models C#3 and R#3 with similar glass beads size of 12-16 US mesh. Use of the estimated thickness of the diffusion-only mass transfer boundary layer decouples the estimation of the oil production rate from the input estimated dispersivity values by equations 42 and 43.

We use the correlation of equation 43 to estimate the applicable inhomogeneity factor and dispersivity values for all of the VAPEX experiments reported by Yazdani and Maini (2005, 2006). For any given experiment with any glass bead size, we use the inhomogeneity factor (Figure 7(a)) and the thickness of the diffusion-only mass transfer BL of the experiment using Model-C#3 with the corresponding glass beads as the reference values. As shown in Figure 6, we use the model to predict the oil production rates for all the VAPEX experiments using the estimated dispersivity values. The model predictions are generally in good agreement with the reported experimental values. For all the experiments, the model predicts the solvent volume fraction of 0.43-0.45 in the produced hydrocarbon mixture which is in agreement with the lab measured values (Yazdani and Maini 2005, 2006).

Effect of Pressure and Temperature on VAPEX Process

The performance of the VAPEX process at given initial reservoir (test) temperature can be enhanced either by increasing the test pressure or by injecting vapour solvent at elevated temperature and pressure conditions. The latter, namely the heated VAPEX process, will result in heat transfer from the vapour phase to the oil in place upon condensation of the injected vapour. Consequently, a draining layer of condensed solvent forms against the interface to which the in place oil leaches and is extracted. The volume of the

condensed solvent in each segment of the interface is dictated by the required heat (provided by the latent heat of the condensed solvent) to advance the heat boundary layer at a given advance rate. The presence of the draining layer of the solvent guarantees the existence of C_o=1 in the mass transfer boundary layer. We investigate the effectiveness of each of these approaches to enhance the process performance using the developed model in the case of butane as the solvent, a typical Athabasca bitumen as the oil, and the dimensions of Model-C#3 with 12-16 glass beads.

The solubility data of C4 in the heavy oil by Yazdani and Maini (2010) and propane in Athabasca bitumen by Badamchi-Zadeh et al. (2009) indicate that the mixtures of light hydrocarbons in the heavy oils are non-ideal and follow the modified version of Raoult's law. Hence, their solubility is reduced by their activity coefficient in the mixture. According to the data by Yazdani and Maini (2010), the maximum solubility of butane in the heavy oil at a test temperature of 22 °C and its dew point pressure of ~220 kPa is ~0.55 by volume fraction.

Figure 8 shows how the predicted oil production rate changes by ~60% as the injection pressure of butane changes from ~200 kPa to ~220 kPa (corresponding to C_o change from 0.46 to 0.55 at the fixed process temperature of 22° C). However, the oil production rate by the heated VAPEX process is almost one order of magnitude greater than the VAPEX process as the injected solvent at elevated temperatures enforces the interface solvent concentration to reach 100% (C_o =1) in the mass transfer boundary layer, illustrated in Figure 9 (a). Figure 8(a) shows that in heated VAPEX cases, the heat transfer BL's contribution to the total oil production rate ($I_T/(I_T+I_C)$) is generally minor (< 10%). Hence, the considerable boost to the oil production rate upon hot vapour solvent injection is due to enhanced mixing within the mass boundary layer by: 1) higher solvent loading; and 2) increased diffusion and dispersion at elevated temperatures as shown in Figure 9(b). Note that the higher solvent loading in drainage layer also improves the mass transfer coefficients. As depicted in Figure 8(b), in the heated VAPEX cases, the liquid hydrocarbon phase drains over a wider thickness of drainage layer with much higher velocities as it is mainly composed of the condensed solvent with lower viscosity. Consequently, the viscous oil is extracted and drained by the draining condensed solvent flow. However, in the VAPEX case, the draining hydrocarbon layer is richer in oil and drains at much lower rates (due to higher viscosity of mixture) over a narrower thickness of the drainage layer.

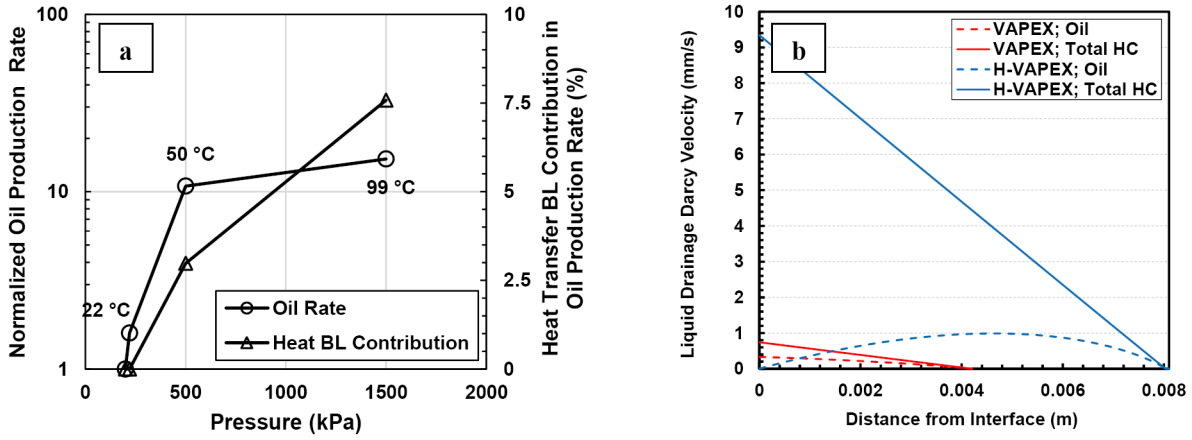

Figure 8—a) The predicted total oil production rate (normalized wrt. the rate of VAPEX at 200 kPa and 22 °C) and contribution of heat transfer BL in VAPEX and heated VAPEX processes in the glass bead pack (Ti=22 °C); 2) Predicted drainage velocities by the model for VAPEX (220 kPa) and heated VAPEX (500 kPa).

Note that the cases studied in this section were presented to demonstrate how the performance of the heated VAPEX process is improved in comparison to the VAPEX process due to differences in the properties of the mass transfer boundary layer. In all these cases, the solvent content within the drainage layer most likely exceeds the onset of the formation of the 2nd heavy liquid hydrocarbon phase by butane. This

phenomena can result in partitioning of up to 25% of the oil to the heavier phase with much higher viscosity than the lighter phase. Hence, the interface will advance as the lighter phase drains but the heavier phase will drain with much smaller rate. This potentially affects the total oil production rate. The quantification of these secondary effects is out of the scope of this paper.

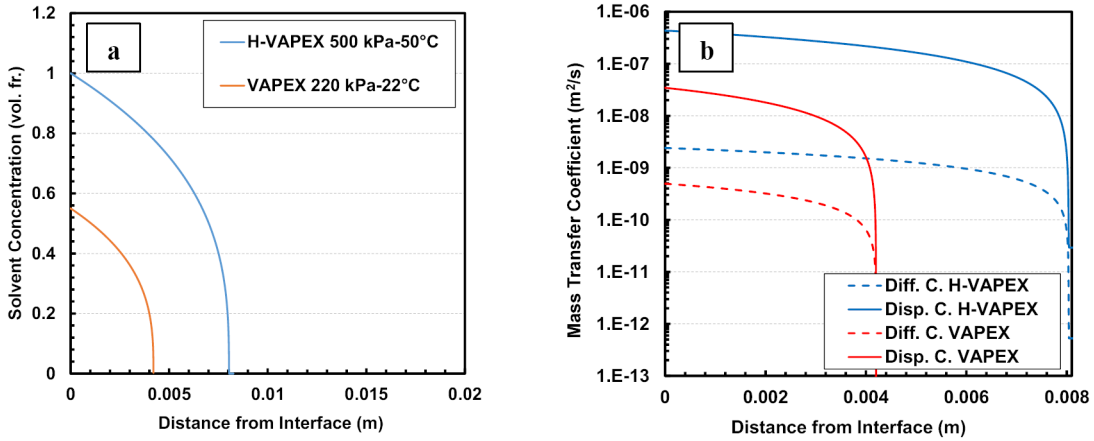

Figure 9—Model predictions of: a) Concentration profile within the mass transfer boundary layer; b) Mass Transfer coefficients within the mass transfer boundary layer, for VAPEX (220 kPa) and heated VAPEX (500 kPa).

H-VAPEX Process Performance in Field-Scale

We investigate the performance of the heated VAPEX process in the field scale using n-pentane as the injected solvent. In general, n-pentane and heavier hydrocarbons are better solvents for this process than the lighter solvents (Khaledi et al. 2018). Among several advantages of n-pentane over lighter HCs are its higher onset concentration to form the 2nd heavy HC liquid phase and lower fractional partitioning of heavy ends of the oil the in the 2nd liquid phase. The injected n-pentane evaporates (Khaledi et al. 2018) the initial water in the reservoir to form an azeotropic vapour mixture with water. The azeotropic vapour mixture condenses on the bitumen interface to deliver heat to the advancing front at a process temperature equal to the azeotropic temperature of the mixture. Hence, it is expected that the water saturation within the drainage layer is higher than the initial water saturation of the reservoir.

The dispersivities values cannot be directly scaled from the lab measurements to the field values as an unconsolidated sand in a typical Athabasca reservoir is different than the glass bead packs by: 1) average grain size and packing heterogeneities; 2) grain size distribution; 3) sphericity and shape of the grains; 4) mixing zone size and geological heterogeneities. Through the analysis of data provided by Perkins and Johnston (1963), a dispersivity value in the order of 0.6-1.8 mm is plausible for sandstones based on the experimental measurements on the outcrops. An approximate up-scaling of the developed correlations of equations 42 and 43 by including all aforementioned factors affecting the packing inhomogeneity results in a dispersivity value of ~1 mm.

Figure 10(a) shows how the predicted oil production rate by the model varies with the input field-scale dispersivity value at the process pressure of 1 MPa. The values are normalized relative to the predicted oil production rate by SAGD at 1 MPa. Assuming no dispersive mixing is present and the diffusion is the only mass transfer mechanisms, the oil production rate by the heated VAPEX process at a temperature of 116 °C is ~70% of the SAGD at the same pressure and steam temperature of 180 °C. Any addition of the dispersive mixing considerably enhances the oil production rate by the heated VAPEX process. Dispersive mixing within the Athabasca sand can potentially boost the oil production rate of the heated VAPEX process up to 240% of the oil rate by SAGD at the same operating pressure. As shown in the Figure 10(b), the dispersive mixing greatly increase the thickness of the drainage layer and increases the solvent loading in

front of the advancing front; hence, it extracts oil by accelerated drainage of the dissolved oil in the drainage condensed solvent bank.

Assuming dispersivity of 1 mm for a typical Athabasca reservoir, we use the model to study the how the operation pressure (and consequently operation temperature) of the heated VAPEX process using pentane affects the oil production rate, Figure 11(a). Not surprisingly the oil rate increases by ~40% as the temperature increase due to higher drainage rates at higher temperatures, shown in Figure 11(b); however, the growth in the contribution of the heat transfer boundary layer is slight, shown in Figure 11 (a). In general, the oil drainage velocities in the heat transfer boundary layer is much lower than the velocities in the mass transfer boundary layer as shown in Figure 11(b). The contribution of drainage within the mass transfer boundary layer, despite being considerably narrower than the heat boundary layer (~0.3 m vs. 7-11 m as shown in Figures 12(a) and 12(b)), is much greater than the heat boundary transfer layer. Hence, the dissolution in and dilution by the condensed solvent significantly enhances the oil production rate in the heated VAPEX process. It is also interesting to note that the thickness of the mass transfer boundary layer does not change significantly as the temperature of the operation changes. Similarly, the total mass transfer coefficient values within the mass boundary layer does not change significantly with a change in the operation temperature as they are mostly dictated by the properties of the solvent-rich drainage layer. However, the limiting values at ξ_C are different due to the difference in the bitumen properties (namely viscosity) at different $T_{\xi C}$. Similar to previous case studies, the total mass transfer coefficient is mainly determined by the dispersion coefficient values as they are 1-2 orders of magnitude greater than the diffusion coefficient. However, the enhanced values of the diffusion coefficient (~10^{-8} m^2/s) at the elevated temperatures in the diluted bitumen mixtures are paramount to establish the transient flow of the draining liquids in order to boost the dispersive mixing mechanisms.

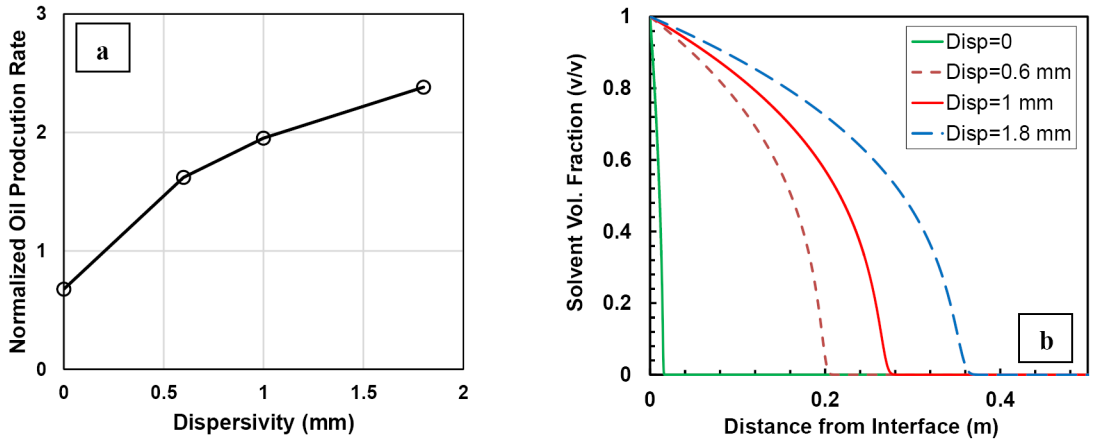

Figure 10—Model predicted: a) oil production rate (normalized wrt. the value SAGD at 1MPa), and b) Concentration profile within the mass transfer boundary layer, versus the input dispersivity for a typical Athabasca in-situ oil sands reservoir in the heated VAPEX process using Pentane at 1 MPa.

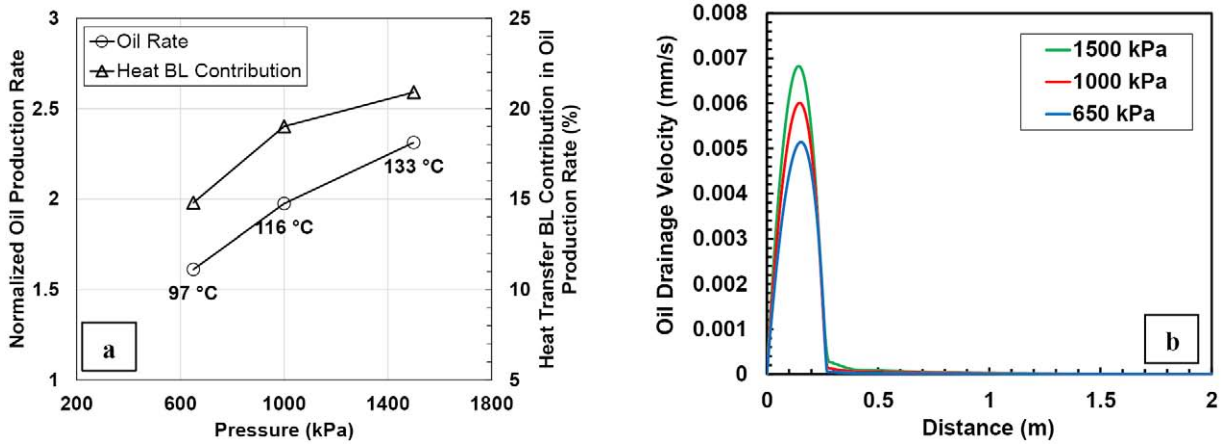

Figure 11—The predicted: a) total oil production rate (normalized wrt. the value SAGD at 1MPa) and contribution of heat transfer BL, and b) oil drainage velocities by the model, in the heated VAPEX process using pentane at different pressures and operating temperatures in a typical Athabasca in-situ oil sands reservoir.

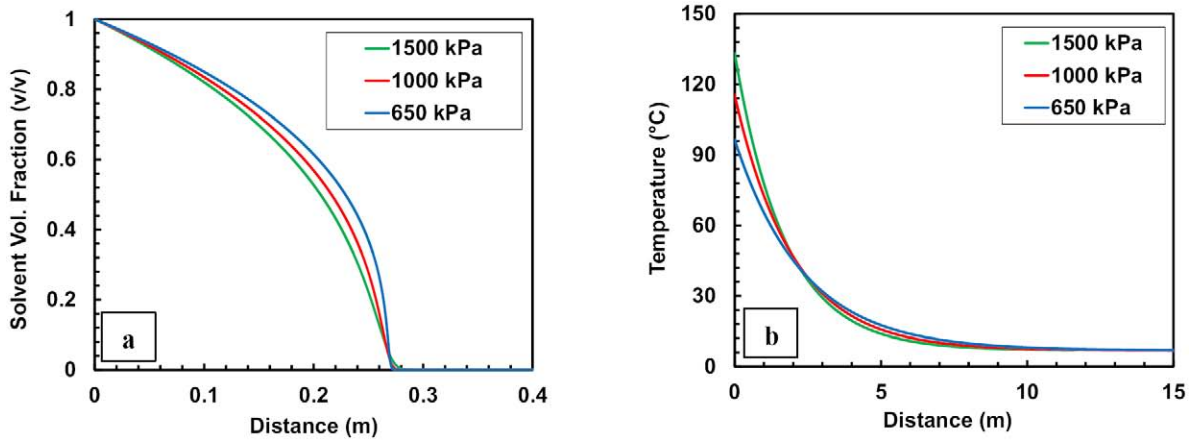

Figure 12—The predicted: a) concentration profile within mass transfer BL, and b) temperature profile in front of advancing front, in the heated VAPEX process using pentane at different pressures and operating temperatures in a typical Athabasca in-situ oil sands reservoir.

Conclusion

A general analytical model was developed for gravity drainage processes by incorporating mass transfer mechanisms (including concentration dependent diffusion and velocity-dependent dispersion) and heat transfer mechanism by conduction. A novel mathematical approach was utilized to analytically solve the second order non-linear partial differential equation governing mass transfer within the mass transfer boundary layer. Mathematical expressions were developed to estimate the concentration and temperature variation within the mass transfer and heat transfer boundary layers, respectively. Explicit equations were provided to calculate the contributions of each boundary layer to total flow within the drainage layer. A closed-form analytical model was also developed to estimate the oil drainage rate due to gravity, heat and dilution effects as a function of reservoir and fluid properties.

The applicability of the developed model was demonstrated by analysis of the experimental data of the VAPEX process from literature. It was shown that, in order to match experimental data, the values of the diffusion coefficients must be inflated to compensate for the dispersion if the dispersive mixing mechanism is excluded in the models. In addition, the inclusion of the concentration-dependent mass transfer coefficients enables the model to predict the concentration profiles in agreement with the experimental observation of the presence of the concentration shock in the VAPEX drainage interface. The scale-dependency of the dispersivity in the porous media packs were investigated using the full dataset of

the VAPEX experiments in different physical model sizes and porous media properties. It was shown that the dispersivity is higher for the packs with smaller grain sizes and its value scales with the size of the mass transfer zone.

The developed model was used to demonstrate how the performance of the VAPEX process is considerably enhanced in the heated VAPEX process in which the vapour solvent is injected at elevated temperature and pressure conditions with respect to the initial temperature and pressure of the reservoir. In the heated VAPEX process, the presence of the draining layer of the condensed solvent results in the enhanced mixing within the mass boundary layer by: 1) higher solvent loading; and 2) increased diffusion and dispersion at elevated temperatures. In general, the in-place viscous heavy oil or bitumen is produced by leaching to the condensed solvent layer which drains with extremely high velocities.

It was also shown that the oil production rate by the heated VAPEX process in a typical Athabasca reservoir can be up to 240% of the oil rate by SAGD at the same operating pressure. The mass transfer boundary layer is generally narrow (~0.3 m) in this process; however, its contribution to the oil production rate can be significantly greater than the heat transfer boundary layer which is thicker by almost one order of magnitude.

The developed model in this work provides a new perspective into the mass transfer mechanisms and their relative importance within the mass transfer boundary layer at different operating conditions. This model can be further improved by the estimation of the local mass transfer coefficients for each segment of the draining layer. One can use a semi-analytical sequential approach (Butler 1985) by dividing the reservoir height to small segments and tracking the location and inclination angle of the interface.

Acknowledgment

The authors thank ExxonMobil and Imperial management for their support and permission to publish this paper.

References

Badamchi-Zadeh, A., Yarranton, H. W., Svrcek, W. Y., & Maini, B. B. (2009, January 1). *Phase Behaviour and Physical Property Measurements for VAPEX Solvents: Part I. Propane and Athabasca Bitumen*. Petroleum Society of Canada. doi:10.2118/09-01-54.

Boone, T.J., Dickson, J.L., and Lu, P. 2014. Development of Solvent and Steam-Solvent Heavy Oil Recovery Processes Through an Integrated Program of Simulation, Laboratory Testing and Field Trials. Presented at 2014 International Petroleum Technology Conference, 10-12 December, Kuala Lumpur, Malaysia. IPTC-18214-MS.

Boone, T.J., Motahhari, H., Khaledi, R. 2015. *Gravity Drainage Process for Recovering Viscous Oil Using Near Azeotropic Injection*. Canadian Patent, CA 2915571.

Boone, T.J., Wattenbarger, C., Clingman, S., Dickson, J.L. 2011. An Integrated Technology Development Plan for Solvent-Based Recovery of Heavy Oil. Presented at 2011 SPE Heavy Oil Conference and Exhibition, 12-14 December, Kuwait City, Kuwait. SPE150706.

Boustani, A., & Maini, B. B. (2001, April 1). *The Role of Diffusion and Convective Dispersion in Vapour Extraction Process*. Petroleum Society of Canada. doi:10.2118/01-04-05.

Butler, R.M. 1979. *Method for Continuously Producing Viscous Hydrocarbons by Gravity Drainage while Injecting Heated Fluids*. Canadian Patent, CA 1130201.

Butler R. M. 1985. A New Approach to the Modeling of Steam-Assisted Gravity Drainage. *Journal of Canadian Petroleum Technology* **24**(3), 42–51.

Butler, R. M., & Stephens, D. J. (1981, April 1). *The Gravity Drainage of Steam-heated Heavy Oil to Parallel Horizontal Wells*. Petroleum Society of Canada. doi:10.2118/81-02-0.

Butler, R. M., and Mokrys, I. J. 1989. Solvent Analog Model of Steam-Assisted Gravity Drainage. *AOSTRA Journal of Research*, **5**(1989) 17, P-17–32 .

Butler, R. M., and Mokrys, I. J. 1991. *A New Process (VAPEX) for Recovering Heavy Oils Using Hot Water and Hydrocarbon Vapour*. JCPT91-01-09.

Butler, R. M., and Mokrys, I. J. 1993. *Recovery of Heavy Oils Using Vapourized Hydrocarbon Solvents: Further Development of the Vapex Process*. JCPT93-06-06

Butler, R.M., McNab, G.S., and Lo, H.Y. 1981. Theoretical Studies on the Gravity Drainage of Heavy Oil during Steam Heating. *Canadian Journal of Chemical Engineering*, Vol. **59**, pp. 455–460.

Das, S. K., Butler, R. M. (1994, January 1). *Investigation of "Vape"x Process in a Packed Cell Using Butane as a Solvent*. Petroleum Society of Canada. doi:10.2118/HWC-94-47.

Das, S. K., Butler, R. M. 1998. Mechanism of the vapour extraction process for heavy oil and bitumen, *In Journal of Petroleum Science and Engineering*, Volume **21**, Issues 1–2, 1998, Pages 43–59, ISSN 0920-4105, https://doi.org/10.1016/S0920-4105(98)00002-3.

Dickson, J.L, Dittaro, L.M, Boone, T.J. 2013a. Integrating the Key Learnings from Laboratory, Simulation, and Field Tests to Assess the Potential for Solvent Assisted - Steam Assisted Gravity Drainage. Presented at 2013 SPE Heavy Oil Conference, 11-13 June, Calgary, Alberta, Canada. SPE 165485.

Dickson, J.L, Subramanian, G., Shah, P., Otahal, J.M., Dittaro, L.M., Jaafar, A.E., Yerian, J.A. 2013b. Key Learnings from a Simulation Study of a Solvent-Assisted SAGD Pilot at Cold Lake. Presented at 2013 SPE Heavy Oil Conference, 11-13 June, Calgary, Alberta, Canada. SPE 165486.

Dittaro, L.M., Jaafar, A.E., Perlau, D.L., Boone, T.J., Yerian, J.A., Dickson, J.L, Wattenbarger, R.C. 2013. Findings from a Solvent-Assisted SAGD Pilot at Cold Lake. Presented at 2013 SPE Heavy Oil Conference, 11-13 June, Calgary, Alberta, Canada. SPE 165434.

Dunn, S. G., Nenniger, E. H. and Rajan, V. S. V. 1989. A study of bitumen recovery by gravity drainage using low temperature soluble gas injection. *Can. J. Chem. Eng.*, **67**: 978–991. doi:10.1002/cjce.5450670617.

Gelhar, L. W., C. Welty, and K. R. Rehfeldt. 1992. A critical review of data on field-scale dispersion in aquifers, *Water Resour. Res.*, **28**(7), 1955–1974, doi:10.1029/92WR00607.

Khaledi, R., Beckman, M., Pustanyk, K., Mohan, A., Wattenbarger, R.C., Dickson, J.L, Boone, T.J. 2012. Physical Modeling of Solvent-Assisted SAGD. Presented at 2012 SPE Heavy Oil Conference, 12-14 June, Calgary, Alberta, Canada. SPE 150676.

Khaledi, R., Boone, T.J., Pustanyk, B.K. 2013. *System and Method for Enhancing Production of Viscous Hydrocarbons from a Subterranean Formation*. Canadian Patent, CA 2886479.

Khaledi, R. Hammouda, A. A., Dittaro, L.M., Dakers, A.P. 2014. Results from a Successful Multi-Year Solvent Assisted SAGD Pilot at Cold Lake. Presented at 2014 World Heavy Oil Congress, 5-7 March, New Orleans, Louisiana, United State of America. WHOC paper 14-157.

Khaledi, R., Pustanyk, B.K, Boone, T.J., Dela Rosa, E.C., Han, W. E. 2014. *Regulation of Asphaltene Production in a Solvent-Based Recovery Process and Selecting of a Composition of a Hydrocarbon Solvent Mixture*. Canadian Patent, CA 2857329.

Khaledi, R., Boone, T.J., Motahhari, H., Subramanian, S. 2015. Optimized Solvent for Solvent Assisted-Steam Assisted Gravity Drainage (SA-SAGD) Recovery Process. Presented at 2015 SPE Heavy Oil Conference, Calgary, Alberta, Canada, SPE-174429.

Khaledi, R., Motahhari, H. 2017. *Recovery of Heavy Oil from a Subterranean Reservoir*. Canadian Patent, CA 2972068, 2017.

Khaledi, R., Motahhari, H., Boone, T. J., Fang, C., Coutee, A. S. 2018. Azeotropic Heated Vapour Extraction- A New Thermal-Solvent Assisted Gravity Drainage Recovery Process. 2018 SPE Heavy Oil Conference, Calgary, Alberta, Canada, SPE-189755.

Leaute, R.P. 2002. Liquid Addition to Steam for Enhancing Recovery (LASER) of Bitumen with CSS: Evolution of Technology from Research Concept to a Field Pilot at Cold Lake. Presented at 2002 SPE International Thermal Operations and Heavy Oil Symposium and International Well Technology Conference, 4-7 November, Calgary, Alberta, SPE-79011.

Mensah-Dartey, R., Lui, Z., Subramanian, S., Boone, T.J., Motahhari, H. 2015. Solvent Assisted Steamflood Study on a Late Life Asset. Presented at World Heavy Oil Congress, Edmonton, Alberta, Canada, paper WHO15-376.

Mokrys, I. J., Butler, R. M. (1993, March 1). *The Rise of Interfering Solvent Chambers: Solvent Analog Model Of Steam-Assisted Gravity Drainage*. Petroleum Society of Canada. doi:10.2118/93-03-02.

Nasr, T. N., Isaacs, E. E. 2001. Process for Enhancing Hydrocarbon Mobility Using a Steam Additive. US patent 6,230,814.

Nenniger, J. E., & Dunn, S. G. (2008, January 1). *How Fast is Solvent Based Gravity Drainage? Petroleum Society of Canada*. doi:10.2118/2008-139.

Oballa, V., Butler, R. M. (1989, March 1). *An Experimental Study of Diffusion In The Bitumen-Toluene System*. Petroleum Society of Canada. doi:10.2118/89-02-03

Okazawa, T. (2007, January 1). *Impacts of Concentration Dependence of Diffusion Coefficient on VAPEX Drainage Rates*. Petroleum Society of Canada. doi:10.2118/2007-170-EA.

Perkins, T. K., & Johnston, O. C. (1963, March 1). A Review of Diffusion and Dispersion in Porous Media. *Society of Petroleum Engineers*. doi:10.2118/480-PA..

Perlau, D.L., Jaafar, A.E., Yerian, J.A. 2011. Novel Design Approached for SA-SAGD Pilot at Cold Lake. Presented at 2011 World Heavy Oil Congress, 14-17 March Edmonton, Alberta, Canada. WHOC paper 11-535.

Stark, D. S. 2013. Cold Lake Commercialization of the Liquid Addition to Steam for Enhancing Recovery (LASER) Process. Presented at International Petroleum Technology Conference, 26-28 March 2013 Beijing, China. IPTC 16795.

Yazdani, A., & Maini, B. B. (2005, June 1). Effect of Height and Grain Size on the Production Rates in the Vapex Process: Experimental Study. *Society of Petroleum Engineers*. doi:10.2118/89409-PA.

Yazdani, A., & Maini, B. B. (2006, January 1). Further Investigation of Drainage Height Effect on Oil Production Rate in Vapex. *Society of Petroleum Engineers*. doi:10.2118/101684-MS.

Yazdani, A., & Maini, B. B. (2010, February 1). Measurements and Modelling of Phase Behaviour and Viscosity of a Heavy Oil/Butane System. *Society of Petroleum Engineers*. doi:10.2118/132484-PA.

Zheng, C. and Bennett, G. D. W. 1995. *Applied Contaminant Transport Modeling; Theory and Practice*, first edition. New York US: van Nostrand Reinhold.

Appendix A

The coefficients γ_k (k=0…7) of the equation 33 are calculated based on the numerical values of the coefficients κ_i (i=0…3) of equation 15 and χ_j (j=0…3) of equation 22 with the following equations:

$$\gamma_0 = \kappa_0.\chi_0$$
$$\gamma_1 = \kappa_1.\chi_0 + \kappa_0.\chi_1 - \kappa_0.\chi_0$$
$$\gamma_2 = \kappa_2.\chi_0 + \kappa_1.\chi_1 + \kappa_0.\chi_2 - \kappa_1.\chi_0 - \kappa_0.\chi_1$$
$$\gamma_3 = \kappa_3.\chi_0 + \kappa_2.\chi_1 + \kappa_1.\chi_2 + \kappa_0.\chi_3 - \kappa_2.\chi_0 - \kappa_1.\chi_1 - \kappa_0.\chi_2$$
$$\gamma_4 = \kappa_3.\chi_1 + \kappa_2.\chi_2 + \kappa_1.\chi_3 - \kappa_3.\chi_0 - \kappa_2.\chi_1 - \kappa_1.\chi_2 - \kappa_0.\chi_3$$
$$\gamma_5 = \kappa_3.\chi_2 + \kappa_2.\chi_3 - \kappa_3.\chi_1 - \kappa_2.\chi_2 - \kappa_1.\chi_3$$
$$\gamma_6 = \kappa_3.\chi_3 - \kappa_3.\chi_2 - \kappa_2.\chi_3$$
$$\gamma_7 = -\kappa_3.\chi_3$$